International Journal of Power Electronics and Drive System (IJPEDS)
Vol. 6, No. 3, September 2015, pp. 423~428
ISSN: 2088-8694

Analysis of Modeling of Current Differential Protection

Denis B. Solovev, Angelina I. Makeeva
Engineering School, Department of Innovatics, Far Eastern Federal University (FEFU), Russian Federation

Article Info

Article history:

Received Mar 21, 2015
Revised May 13, 2015
Accepted Jun 5, 2015

Keyword:

Busbar protection
Current transformers
Differential protection
Rogowsky coils
Transient simulation

ABSTRACT

Analysis of transients in longitudinal differential protection schemes is given basing on results obtained by simulation. Simulation diagram for modeling differential protection with current transformers with non-linear cores is proposed. Main shortcomings of using current transformers as measuring transducers are shown. Solutions of the problem revealed are proposed.

Corresponding Author:

Denis B. Solovev,
Engineering school, Department of Innovatics,
Far Eastern Federal University (FEFU),
City of Vladivostok, Russky Island, Russian Federation.
Email: solovev.db@dvfu.ru

1. INTRODUCTION

Current differential protections are protections with absolute selectivity comparing currents either at the terminals of an element to be protected or in parallel circuits of electric installations. The first type of such protections is called longitudinal current differential protection while the other – transverse differential protection [1–2].

Transverse differential protection controls the equality of currents in parallel transmission lines or parallel branches of windings in large transformers or rotating machines. Longitudinal differential protection is more widespread than the transverse one. It is used for protection of lines, busbars, reactors, and windings of transformers and other electric machines. That is why only longitudinal protection is discussed below.

In most existing differential protections measurement of currents is done with current transformers (CTs). The CTs connected at the terminals of protected element must have identical parameters such as rated values of primary and secondary currents, core sizes, and core material. The exceptions with the rule are differential protections of transformers where CTs installed on HV, MV, and LV sides of the transformer have different transformation ratios. Implementation features of transformer differential protections are well known from course books [1–2] and not discussed in this article.

2. THE PROPOSED METHOD

Current differential protections are usually based on the scheme with circulating currents. In this case the secondary windings of the CTs on the terminals of the protected element are connected to the relay terminals so that the secondary currents of these CTs are in opposite direction relative to the relay terminals [1–2].

During normal operation of the protected element when currents at its ends are equal and fall within the rated range the secondary currents of both CTs are approximately equal. The current flowing through the relay is called "imbalance current". It is negligibly small and is determined by the difference between the magnetizing currents of the CTs. This difference is caused by some difference between the parameters of their cores at low e.m.f. of the secondary windings.

In case of insulation fault in the protected element short circuit current i_{SC} starts to flow from the faulty element to the earth or other phases, and the primary currents of the CTs become unequal. As a result the imbalance current, i_p, flows through the relay. It is approximately equal to i_{SC}/n, where n is the CT transformation ratio.

The imbalance current also appears if due to a short circuit outside the protected element high currents flow through the element. In this case the primary currents of both the CTs are equal and cause saturation of the CT cores. As the saturation curves of the cores cannot be fully coincident imbalance current will flow through the relay. This current will be equal to algebraic difference of CT magnetizing current instantaneous values [3]. The order of this current is determined by the overcurrent ratio and the mismatch of the CT magnetizing curves.

3. RESEARCH METHOD

Let us discuss the results of simulation of a transient in longitudinal differential protection in case of short circuit that is external relative to the element protected. The scheme used for simulation of the protection in Micro-Cap environment [4] is shown in Figure 1.

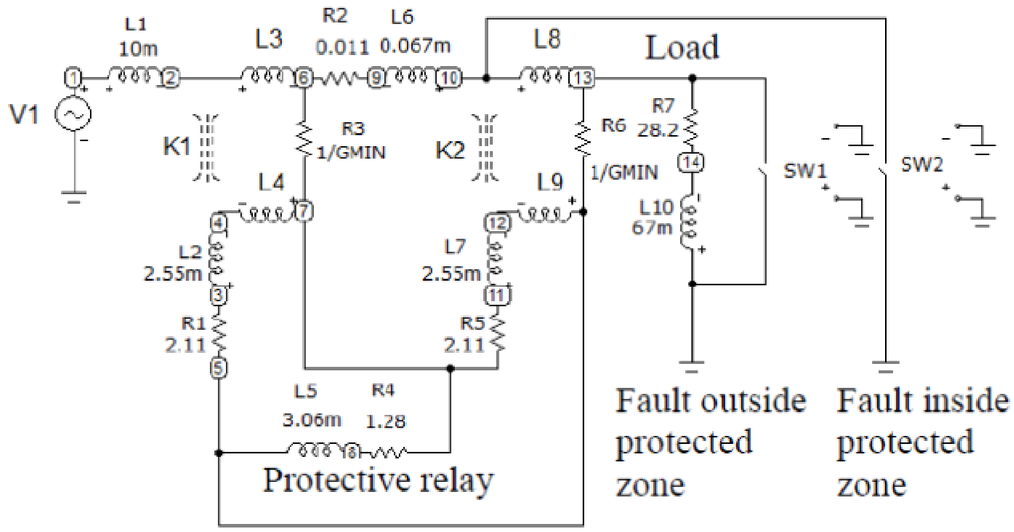

Figure 1. Simulation diagram of longitudinal differential protection using CTs with non-linear cores

The simulated circuit represents current differential protection of HV aerial line of 220 kV power network. The protected element is represented by substitution circuit including serially connected resistor R2 (R=0,011 Ohm) and inductor L6 (L=0,067 mH). The current transformer installed at the beginning of the line, CT1, is simulated as two inductances, L3 and L4, that are inductively coupled through non-linear core K1. The stray inductance of CT1 secondary winding and its ohmic resistance are represented by elements L2 and R1. The parameters of these elements and the core of the CT are as follows:

- mean length of magnetic flux line of the core – 2,66 m (PATH = 266 cm);
- core cross-section – $6{,}0 \cdot 10^{-4}$ m^2 (AREA = 6 cm^2);
- ohmic resistance of secondary winding – R_2 = 2,11 Ohm;
- reactance and stray inductance of secondary winding – X_2 = 0,8 Ohm and L_2 = 2,55 mH;
- domain walls irreversible deformation constant – K = 25 A/m [1–2].;
- domain border elastic displacement constant – C = 0,001 [1–2].

It is presumed that the core of transformer CT1 is made of steel 3411 of better grade. According to data given in [5] such steel has the following parameters: saturation magnetization MS$_1$ = $1{,}53 \cdot 10^6$ A/m, and hysteresisless magnetization curve form factor A_1 = 174 A/m. These parameters are used for simulation of the magnetic core in *Micro-Cap* environment.

The current transformer installed at the end of the line, CT2, is simulated as two inductances, L8 and L9, that are inductively coupled through non-linear core K1. It is presumed that the core of transformer CT2 is made of steel 3411 of worse grade. According to data given in [5] such steel has the following parameters: saturation magnetization $MS_1 = 1{,}31\cdot10^6$ A/m, and hysteresisless magnetization curve form factor A_1 = 166 A/m. Other parameters of CT2 are similar to those of CT1.

In accordance with recommendations of *Micro-Cap* the inductive elements of the transformers are connected via resistors R3 and R6 whose resistance is denoted as 1/GMIN (i.e. 10^{12} Ohm).

According to the scheme of circulating current differential protection the secondary windings of CT1 and CT2 form a loop of elements L4, L2, R1, L9, L7, R5. The ends of the windings are connected to common nodes 5 and 7. The relay connected to the same nodes actuates the tripping circuit of the circuit breaker powering the protected line. In the simulated circuit the relay is represented by serially-connected inductor L5 (L=3,06 mH) and resistor R4 (R=1,28 Ohm).

The load connected to the end of the line is simulated as inductor L10 (67 mH) and resistor R7 (28,2 Ohm).

In the simulation diagram shown in Figure 1 the sinusoidal voltage source, V1, has the following parameters: voltage amplitude – $\sqrt{2}\cdot220000/\sqrt{3}$ V, frequency –50 Hz, source internal resistance - 0,17 Ohm (this value is entered into the box of setting parameters of source V1 along with voltage amplitude and frequency), and source internal reactance X_1 = 3,17 Ohm. In the simulation diagram the reactive component corresponding to the last value is represented by element L1 having inductance of 10 mH.

Resistance of R2 and inductance of L6 representing the protected line are negligibly small when compared to the values of R7 and L10 representing the load connected to the end of the line. The steady-state load current is 3,46 kA, that is 86,5% of the rated current of the CT primary winding. The r.m.s. value of the short circuit current periodic component is 40 kA.

The simulated short circuit process occurs after making of either of the two circuit breakers (SW1 or SW2). For each of them making time and resistance in closed and open conditions are set. The corresponding values of these resistances are set to 0,001 Ohm and 1 MOhm.

During simulation of the *short circuit process within the protected zone* the switch SW1 closure time is set to a value exceeding the duration of the transient, so the switch remains open for the whole simulation time. The closure time of switch SW2 for this mode is assumed to be 0,04 s. By this time the load energizing transient will start (at time equal to zero) and virtually terminate. At t = 0,04 s a short circuit in the protected zone occurs. In this case the initial value of the aperiodic component of the short circuit current is close to the amplitude of the periodic component thereof while the maximum fault current will be reached in approximately 0,01 s after beginning of the process. This maximum will be approximately equal to the maximum possible value i.e. the inrush short-circuit current. During the whole simulation time switch SW2 remains in the closed state.

The results of simulation of transients during energizing of the load and subsequent short circuit in the protected zone are shown in Figure 2. In Figure 2, *a* are shown the curves of the following variables: source current I (L1) that is almost equal to current I (L3) of CT1 primary winding (load and subsequent short-circuit current) and imbalance current (relay current) I (L5) while in Figure 2, b – currents I (L4) and I (L9) of CT1 and CT2 secondary windings. The imbalance current is shown inverted to simplify visual comparison of this current with the CT secondary currents.

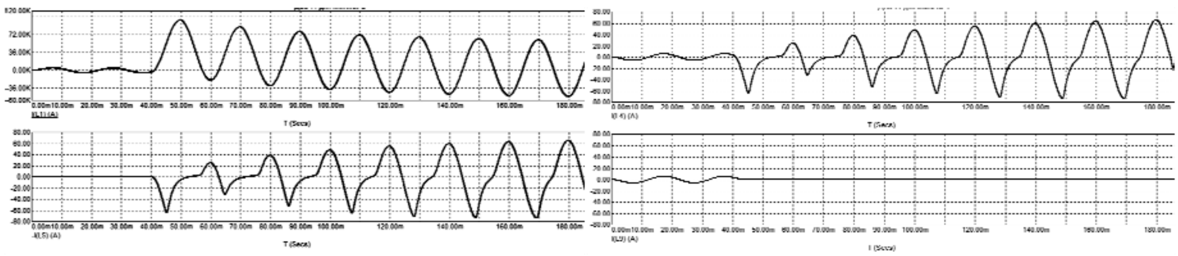

a) b)

a) waveforms of source I (L1) and imbalance I (L5) currents;
b) waveforms of currents I (L4) and I (L9) of CT1 and CT2 secondary windings

Figure 2. Energizing of load and subsequent short circuit in the protected zone

As it can be seen, in the interval from 0 s to 0,04 s load energization process occurs with the amplitude of the forced component being 4,9 kA . The secondary currents of CT1 and CT2 are practically equal. The amplitude of the forced component of these currents is 6,1 kA. The imbalance current stays equal to zero. At instant t = 0,04 s the short circuit occurs. The amplitude of the forced component of the short circuit current is 85 kA. It reaches its maximum (101,5 kA) in half a period (at t = 0,05 s).

Then the secondary current of CT2 becomes close to zero. The absolute values of the imbalance current and CT1 secondary current are close to each other (the first peak of the secondary current is 63,7 A while that of the imbalance current – 63,6 A).

Almost all of secondary current of CT1 flows through the relay due to high impedance of CT2 secondary winding. It results from the fact that current does not flow through CT2 primary winding and its core is demagnetized so the reactance of CT2 magnetizing loop is much higher than the leakage reactance of the secondary winding as well as its resistance.

The current waveform of CT2 secondary winding and the relay is highly distorted. As the aperiodic component decays the waveform of these currents improves but remains clearly non-sinusoidal. Such distortions are caused by deep saturation of CT1 core. Eventually the positive and negative peaks of imbalance current and CT1 secondary current equalize and become close to the values of 69,2 A and 69,3 A. The imbalance current considerably exceeds the rated value of CT secondary current (5 A), so the relay must operate and disconnect the protected line from the source.

In Figure 3 are shown the results of simulation of load energizing and consequent *short circuit outside the protected zone*. In this case circuit breaker SW1 will close at t = 0,04 s and short circuit will occur outside the protected zone. The circuit breaker SW2 remains open for the whole time.

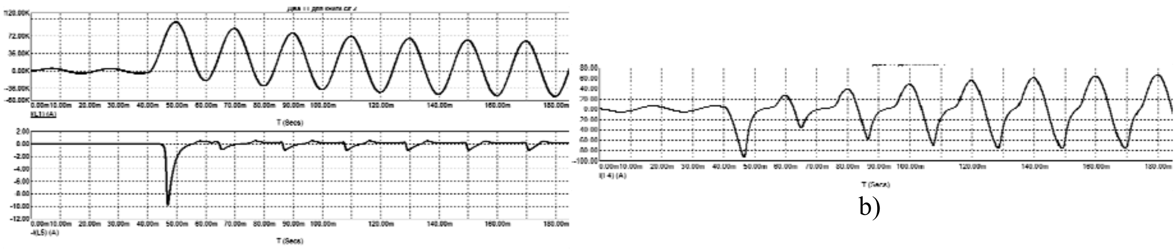

b)

a)

a) source current I (L1) and imbalance current I (L5);
b) CT1 secondary current I (L4).

Figure 3. Waveforms at load energization with subsequent fault outside the protected zone

In Figure 3 are shown waveforms of the following variables: source current I (L1) (Figure 3, a), imbalance current I (L5) (Figure 3, a), and CT1 secondary current I (L4) (Figure 3, b).

As in Figure 2 it can be seen that in the interval from 0 s to 0,04 s load energization process occurs with the amplitude of the forced component being 4,9 kA. The secondary currents of CT1 and CT2 are practically equal. The amplitude of the forced component of these currents is 6,1 kA. The imbalance current stays equal to zero. At instant t = 0,04 s the short circuit occurs. The amplitude of the forced component of the short circuit current is 85 kA. It reaches its maximum (101,5 kA) in half a period (at t = 0,05 s).

If both the CTs had cores with fully identical parameters the secondary currents of CT1 and CT2 would be the same and the imbalance current would be zero both in case of external fault and at load. However during short circuit the primary currents are higher that at proceeding load, so the cores of CT1 and CT2 saturate. Their magnetizing currents rise but to different extents. The magnetizing current of CT2 rises to a higher value as CT2 core is made of steel of worse grade. Therefore the secondary current of CT1 becomes higher than that of CT2. In this case there appears noticeable difference of these currents caused by the measurement error of the differential protection. This difference results in non-zero imbalance current. This current has the appearance of alternating short pulses with waveform close to triangular. The first pulse has negative polarity and the largest amplitude of 9,8 A. The following pulse has positive polarity and the least amplitude not exceeding 0,1 A. Eventually the amplitudes of positive pulses rise while those of negative pulses fade. By approximately 0,2 s the amplitude of negative pulses falls to 1 A. Then the amplitudes of positive and negative pulses equalize at level of about 0,1 A.

The obtained result shows that the current differential protection has the following shortcoming. It can give false trips at high fault currents caused by short circuits occurring outside the protected zone even if the currents at both ends of the protected element are equal.

To avoid such false trips (at such faults overcurrent protection should operate) a delay may be introduced to avoid tripping the protected element by the first pulse having the largest amplitude. Also, the sensitivity of the protection may be reduced. The protection should not operate at relatively low pulses after the delay elapses. The protection with reduced sensitivity will not trip the protected element until the insulation breakdown does not develop and the fault current becomes higher than the operation threshold. In this case the damage caused by the short circuit current will be considerably higher than in case of tripping at the first stage of insulation fault development.

As can be seen from Figure 4 the current measurement error of the differential protection considerably rises in the following situation. In the beginning a short circuit in the protected zone occurs. After it has been cleared another short circuit outside the protected zone occurs. The time interval between the two faults is not enough for the CT cores to demagnetize. So before the beginning of the second fault the cores have remanent magnetization. As a result the cores become more saturated causing the measurement error (imbalance current) and the false trip probability to rise.

As in the first case (Figure 2) short circuit in the protected zone (between CT1 and CT2) occurs after 0,04 s from energization of the load. At instant t = 0,08342 s this fault was cleared. This instant corresponds to zero crossing of the short circuit current. Selection of such fault clearance time simplifies the simulation diagram as in this case it is not necessary to introduce elements representing processes caused by electric arc during tripping the circuit breaker.

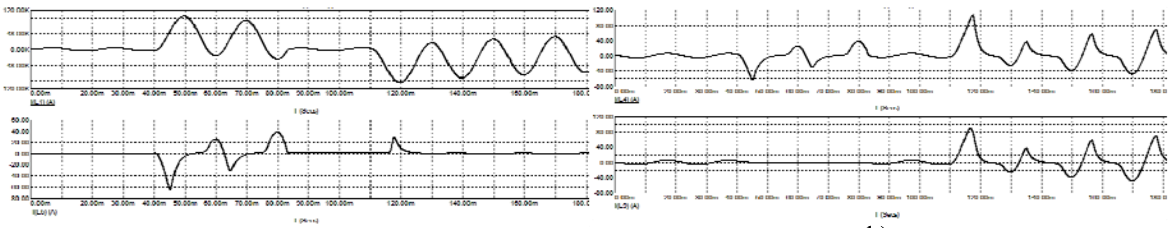

a) b)

a) source current I (L1) and imbalance current I (L5);
b) currents I (L4) and I (L9) of CT1 and CT2 secondary windings.

Figure 4. Clearing fault outside protected zone after clearing fault within protected zone

At instant t = 0,11 s new short circuit occurs behind CT2. It can be seen that the second short-circuit current has negative aperiodic component i.e. its polarity is inverse as compared to such component of the first short circuit current.

During the first fault the imbalance current appears at the same time and has the same waveform and instantaneous values as in the first case (Figure 2). During the second fault the waveform of the first imbalance current pulse is similar to that in the second case (Figure 3). But the amplitude of this pulse is 28,7 A instead of 9,8 A that is almost three times higher. Then as in the second case the amplitudes of negative and positive imbalance current pulses equalize at level of 0,1 A after rather long time.

The simulated imbalance current waveforms obtained for faults outside the protected zone involving deep saturation of the CT cores are similar to the imbalance current waveform given in [3]. These waveforms were calculated by computer using approximation of the CT core magnetization curve with three straight segments i.e. without consideration of the hysteresis. Use of Micro-Cap environment with the same purpose greatly simplifies the calculations and provides better accuracy.

4. DISCUSSION

For increasing the sensitivity of current differential protection and reduction of false operation probability in case of faults outside the protected zone a number of methods was offered [5] e.g. use of a relay with saturable current transformer. In this case the sensitivity is reduced during action of the aperiodic component of imbalance current. The other way to reduce the influence of high currents during external faults is to use current differential relays with magnetic restraint or restraint based on electronics.

The using of the discussed methods results in complication of differential protection devices and deterioration of their response time.

5. CONCLUSION

The above shortcomings can be overcome by use of some innovative solutions e.g. by replacement of CTs for Rogowsky coils avoiding use of integrating filters [6-10]. In this case the weight of the current transducers is greatly reduced and the protection device schematic is simplified. The probability of false trips is also greatly reduced as Rogowsky coils do not saturate. Besides the impact of aperiodic components of the measured currents is reduced as the derivative of such components is much smaller than the amplitude values of the periodic components (Rogowsky coils measure derivatives of currents instead of currents as such).

REFERENCES

[1] S. H. Horowitz, *et al.*, "Power System Relaying", Third Edition, John Wiley & Sons, Ltd, Chichester, UK, ISBN: 978-047-07-5878-6; 2008. http://dx.doi.org/ 10.1002/9780470758786.ch7.

[2] "Power System Protection: Principles and components". Editor: Electricity Training Association, UK, ISBN: 978-184-91-9442-6; 1995. http://dx.doi.org/10.1049/PBPO905F.

[3] A. Wright, *et al.,* "Electrical Power System Protection", Publisher Springer US, ISBN: 978-1-4615-3072-5; 1993. http://dx.doi.org/10.1007/978-1-4615-3072-5. Available from: http://link.springer.com/book/10.1007/978-1-4615-3072-5.

[4] Spectrum-soft. http://www.spectrum-soft.com/index.shtm.

[5] A. Wright, Current Transformers: Their Transient and Steady-state Performance (Modern Electrical Studies). Publisher: Chapman and Hall; 1St Edition edition. ISBN: 978-0-4120-8850-6; 1968. http: http://www.amazon.com/Current-Transformers-Steady-state-Performance-Electrical/dp/0412088509.

[6] L. Kojovic, "Rogowski Coils Suit Relay Protection and Measurement", *IEEE Computer Applications in Power*, Vol. 10, No. 3, pp. 47-52, July 1997. http://dx.doi.org/ 10.1109/67.595293.

[7] L. Kojovic, "PCB Rogowski coils benefit relay protection", *IEEE Computer Applications in Power*, vol. 15. pp. 50–53, 2002. http://dx.doi.org/ 10.1109/MCAP.2002.1018823.

[8] D. B. Solovev, *et al.,* "Instrument current transducers with Rogowski coils in protective relaying applications", *International Journal of Electrical Power and Energy Systems*, Vol. 73C, pp. 107-113, 2015. http://dx.doi.org/ 10.1016/j.ijepes.2015.04.011.

[9] P. Petit, *et al.,* "Basic MOSFET Based vs Couplecoils Boost Converters for Photovoltaic Generators", *International Journal of Power Electronics and Drive Systems (IJPEDS)*, Vol. 4, pp. 1-11, 2014.

[10] P. Li, *et al.,* "High Frequency Characteristic Of Rogowski Coil", *TELKOMNIKA Indonesian Journal of Electrical Engineering*, Vol. 10, pp. 2209-2214, 2012.

BIOGRAPHIES OF AUTHORS

Denis B. Solovev is a graduate of Far Eastern State Technical University (Diploma with honours), Vladivostok, Russia. In 2011 he received a PhD in electric engineering. From 2011 to 2015 he took internship in the leading Russian and international universities and research laboratories: MATI - Russian State Technological University named after K.E. Tsiolkovsky, Moscow; University of Maastricht, Maastricht (Netherlands); Laboratory of the Ministry of Energy of the United States of America, Seattle and Richland, Washington. He is currently the head of the educational program "Innovatica" (cluster of energy and electronics) at the Engineering School of the Far Eastern Federal University, Vladivostok, Russia.

Angelina I. Makeeva student of chair "Innovatica" (cluster of energy and electronics) at the Engineering School of the Far Eastern Federal University, Vladivostok, Russia.